

Exact transverse solitary and periodic wave solutions in a coupled nonlinear inductor-capacitor network

Serge Bruno Yamgoué, Guy Roger Deffo, Eric Tala-Tebue, François Beceau Pelap

Citation: Chin. Phys. B . 2018, 27(9): 096301. **doi:** 10.1088/1674-1056/27/9/096301

Journal homepage: http://cpb.iphy.ac.cn; http://iopscience.iop.org/cpb

What follows is a list of articles you may be interested in

Discrete breathers in a model with Morse potentials

Lü Bin-Bin, Deng Yan-Ping, Tian Qiang

Chin. Phys. B . 2010, 19(2): 026302. **doi:** 10.1088/1674-1056/19/2/026302

Exact transverse solitary and periodic wave solutions in a coupled nonlinear inductor–capacitor network

Serge Bruno Yamgoué[1,†], Guy Roger Deffo[2], Eric Tala-Tebue[3], and François Beceau Pelap[2]

[1] *Department of Physics, Higher Teacher Training College Bambili, the University of Bamenda, P.O. Box* 39 *Bamenda, Cameroon*
[2] *Unité de Recherche de Mécanique et de Modélisation des Systèmes Physiques (UR-2MSP), Faculté des Sciences, Université de Dschang, BP* 69 *Dschang, Cameroun*
[3] *Department of Telecommunication and Network Engineering, Fotso Victor University Institute of Technology, The University of Dschang, P.O. Box* 134, *Bandjoun, Cameroon*

(Received 14 May 2018; revised manuscript received 29 May 2018; published online 28 August 2018)

Through two methods, we investigate the solitary and periodic wave solutions of the differential equation describing a nonlinear coupled two-dimensional discrete electrical lattice. The fixed points of our model equation are examined and the bifurcations of phase portraits of this equation for various values of the front wave velocity are presented. Using the sine-Gordon expansion method and classic integration, we obtain exact transverse solutions including breathers, bright solitons, and periodic solutions.

Keywords: nonlinear electrical lattices, two-dimensional network, sine-Gordon expansion, exact transverse solitary wave solutions

PACS: 63.20.Pw **DOI:** 10.1088/1674-1056/27/9/096301

1. Introduction

The responses of nonlinear dispersive systems and their applications are fascinating subjects that are currently at the forefront of research in nonlinear optics,[1–4] plasma physics,[5,6] biology,[7] atomic chains,[8–11] Fermi–Pasta–Ulam lattices,[12–14], crystals,[15–19] and discrete electrical transmission lines[20–27] to mention just a few. Depending on the fields, several elements are at the origin of the nonlinear and dispersive character of these systems. In the case of electrical transmission lines (NLTL), for example, nonlinear and dispersion effects are introduced by nonlinear capacitors and linear inductors, respectively.

The combined effects of these two phenomena are capable of generating solitary waves in the system. The energy of such waves is localized in space and they are extremely stable during their propagation.[28] Several types have been studied. These solutions exist on several forms[29–32] and are shape-preserving in the nonlinear dispersive media through which they are propagated. They are very significant in diverse fields of physics and engineering. In modern textile engineering, for instance, non-linear differential-difference equations with soliton solutions are often used to describe some phenomena arising in heat/electron conduction and flow in carbon nanotubes.[33] Thus, soliton solutions and their interactions are theoretically investigated in various nonlinear evolutions equations such as the coupled KdV equations with variable coefficients,[34] the $(2+1)$-dimensional generalized fifth-order KdV equation,[35] the modified Zakharov–Kuznetsov equation,[36] the standard nonlinear Schrodinger equation and its extended forms,[37–41] the $(2+1)$-dimensional Ito equation,[42] the Kadomtsev–Petviashvili equation and its B-type,[43–45] to name just a few. There is equally a great deal of interest devoted to experimental investigations on solitons. This is conspicuously illustrated, for example, by the very recent paper by Liu *et al.*[46] and the large number of references therein on similarly works.

In the literature, many powerful methods have been developed by mathematicians and physicists to tackle the complexity of these model equations. Most of those methods have in common the fact that they assume the solutions in the form of an expansion, generally polynomial, in terms of an auxiliary function. The latter is usually (constructed from) the solution of some explicitly integrable ordinary differential equations (ODEs). Such an idea was presented earlier in solving the the Kolmogorov–Petrovskii–Piskunov equation[47] and later developed into a systematical approach, called the transformed rational function method.[48] Several variants of this approach can be distinguished depending on the specific auxiliary function. They include the G'/G-expansion method,[49–51] the exp-expansion method,[52,53] the extended F-expansion method,[54] the tanh method,[55,56] the Jacobi elliptic function rational expansion method,[57] the generalized Riccati equation mapping method,[58] the bifurcation method of dynamical system,[59–63] and the sine-Gordon expansion-method,[64–66] among others. It is important to point out that, when several of these methods are applicable to a given equation, they lead to different forms of solutions that are however equivalent to one another; see Ref. [67] for a related discus-

†Corresponding author. E-mail: sergebruno@yahoo.fr

© 2018 Chinese Physical Society and IOP Publishing Ltd

sion.

The sine-Gordon expansion-method is currently one of the most attractive techniques for solving nonlinear evolution equations. Baskonus *et al.* have recently employed it to obtain the new solitary wave solutions to the $(2+1)$-dimensional Calogero–Bogoyavlenskii–Schiff and Kadomtsev–Petviashvili hierarchy equations.[68] More recently, this method has been utilized to investigate the solitary wave solutions of a nonlinear model arising in plasma physics[69] and in nonlinear sciences.[70]

In this study, we apply the same powerful sine-Gordon expansion method (SGEM) and classic integration to analyze the dynamics of transverse traveling waves in a two-dimensional nonlinear electrical transmission line. The paper is organized as follows. In Section 2, our electrical network model is presented along with the set of discrete ordinary differential equations (ODE) governing its dynamics. The latter is afterwards reduced first to a system of two coupled partial differential equations under the long wavelength approximation, and finally to an ODE by means of some transformations. Section 3 is devoted to the dynamical studies of that ODE in the first part and to the outline of the SGEM in the second part. In Section 4, using SGEM and classic integration, the exact analytical expressions of solitary and periodic waves solutions are obtained and their profiles are portrayed. Some physically exploitable solutions in the particular case of our electrical network are given in Section 5. We conclude our paper in Section 6.

2. Model description and dynamic equation

We consider a coupled nonlinear transmission line which consists of a number of *LC* blocks connected as illustrated in Fig. 1. The nodes in the system are labeled with two discrete coordinates n and m which specify the nodes in two mutually perpendicular directions. In these two directions, the inductance and the capacitance are different, being (L_1, C_1) and (L_2, C_2), respectively.

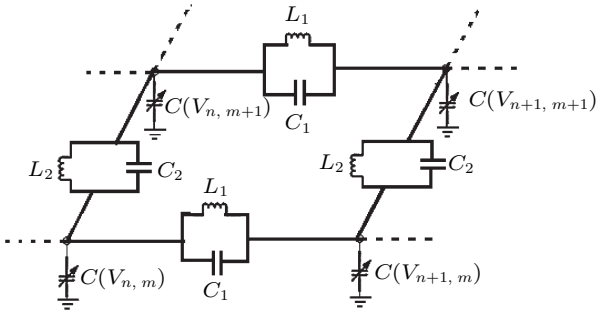


Fig. 1. Schematic representation of the nonlinear transmission line.

The electric charge relationship function of voltage $V_{n,m}$ can be approximated by a second-order polynomial[71–74]

$$Q_{n,m} = C_0\left(V_{n,m} - \alpha V_{n,m}^2\right), \tag{1}$$

where C_0 is the characteristic capacitance while the nonlinearity coefficient α is a positive constant. Applying Kirchhoff laws to this circuit leads to the following set of differential equations governing the dynamics of voltage signals in the network:

$$\begin{aligned}
&\frac{\mathrm{d}^2 V_{n,m}}{\mathrm{d}t^2} - \alpha\frac{\mathrm{d}^2 V_{n,m}^2}{\mathrm{d}t^2} + u_{01}^2\left(2V_{n,n} - V_{n+1,m} - V_{n-1,m}\right)\\
&+ u_{02}^2\left(2V_{n,m} - V_{n,m+1} - V_{n,m-1}\right)\\
&= C_{\mathrm{r}1}\frac{\mathrm{d}^2}{\mathrm{d}t^2}\left(V_{n-1,m} + V_{n+1,m} - 2V_{n,m}\right)\\
&+ C_{\mathrm{r}2}\frac{\mathrm{d}^2}{\mathrm{d}t^2}\left(V_{n,m-1} + V_{n,m+1} - 2V_{n,m}\right),
\end{aligned} \tag{2}$$

with $n = 1,2,\ldots,N$, $m = 1,2,\ldots,M$, $u_{01}^2 = 1/L_1C_0$, $u_{02}^2 = 1/L_2C_0$, $C_{\mathrm{r}1} = C_1/C_0$, and $C_{\mathrm{r}2} = C_2/C_0$. Here, N and M are the numbers of cells considered in directions n and m, respectively.

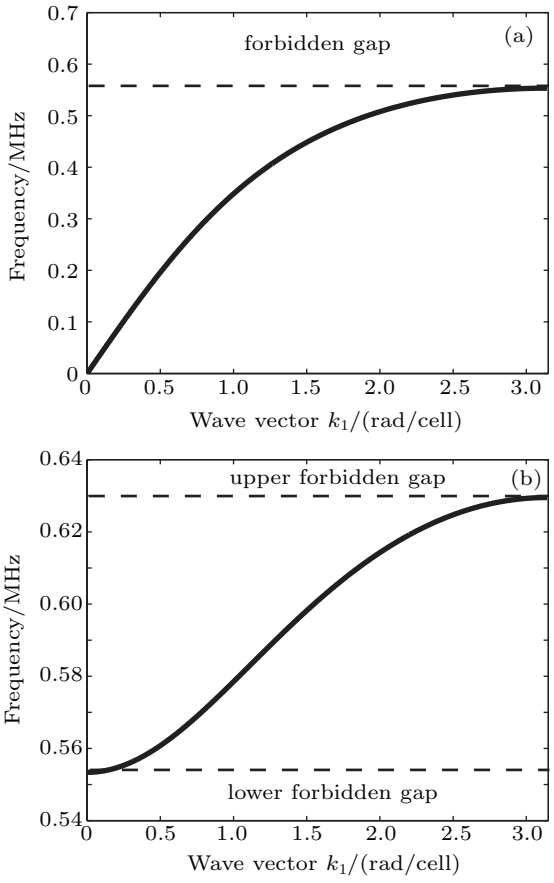


Fig. 2. The linear dispersion of the network according of the wave vector k_1 (rad/cell) for $u_{01} = 2.5786\times10^6$ rad/s, $u_{02} = 2.5786\times10^6$ rad/s, $C_{\mathrm{r}1} = 0.3$, and $C_{\mathrm{r}2} = 0.3$: (a) $k_2 = 0$ and (b) $k_2 = \pi$.

The corresponding linear dispersion law describing small amplitude waves of the form $A_0\exp(\mathrm{i}(k_1n + k_2m - \omega t))$ is

given by

$$\omega^2 = \frac{4u_{01}^2 \sin^2(\frac{k_1}{2}) + 4u_{02}^2 \sin^2(\frac{k_2}{2})}{1 + 4C_{r1} \sin^2(\frac{k_1}{2}) + 4C_{r2} \sin^2(\frac{k_2}{2})}. \quad (3)$$

This dispersion relation shows that our network is a band-pass filter with the cutoff frequency $\omega_c^2 = \frac{4u_{01}^2+4u_{02}^2}{1+4C_{r1}+4C_{r2}}$. For values of k_i chosen in the Brillouin zone ($0 < k_i < \pi$) with $i = 1, 2$, we present the evolution of the angular frequency for the n direction and for two specific values of transversal wave numbers k_2 in Fig. 2.

The discreteness and nonlinearity of these coupled ODEs render their exact analytical investigation obviously intractable. To manage this difficulty, we can use the continuum approximation by setting $V_{n,m}(t) \longrightarrow V(n,m,t)$. We suppose that the spacing between two adjacent sections is the same in the two directions ($h_1 = h_2 = h$). To express the space variables n and m in units of cell, the lattice spacing h is taken as equal to one. Then, using this approximation, we obtain from Eq. (2) the following two-dimensional partial differential equation (PDE) for the perturbed voltage V:

$$\frac{d^2}{dt^2}(V - \alpha V^2) - u_{01}^2 \frac{\partial^2 V}{\partial n^2} - u_{02}^2 \frac{\partial^2 V}{\partial m^2} - C_{r1} \frac{d^2}{dt^2}\left(\frac{\partial^2 V}{\partial n^2}\right) - C_{r2} \frac{d^2}{dt^2}\left(\frac{\partial^2 V}{\partial m^2}\right) = 0. \quad (4)$$

To find the traveling wave solutions of this equation we introduce the Gardner-Morikawa transformation of the independent variables. This specific transformation is widely used for the analytical investigation of nonlinear discrete lattices[25,39,75,76] owing to its feature of properly balancing the nonlinearity and dispersion after expansion. For our two-dimensional network, it reads

$$V = \epsilon \psi(x, y, \tau), \quad x = \epsilon^{\frac{1}{2}}(n - \upsilon_1 t), \quad y = \epsilon^{\frac{1}{2}}(m - \upsilon_2 t), \quad \tau = \epsilon^{\frac{3}{2}} t, \quad (5)$$

where $\epsilon \ll 1$ is a formal parameter while x and y are the instantaneous coordinates of the moving structure in the network. Correspondingly, υ_1 and υ_2 are the components of the displacement velocity in these respective directions. The use of these variables also implies that the time and space derivative operators are transformed according to

$$\frac{d}{dt} = \epsilon^{\frac{3}{2}} \frac{\partial}{\partial \tau} - \epsilon^{\frac{1}{2}} \upsilon_1 \frac{\partial}{\partial x} - \epsilon^{\frac{1}{2}} \upsilon_2 \frac{\partial}{\partial y}, \quad (6)$$

$$\frac{d^2}{dt^2} = \epsilon^2 \left(\upsilon_1 \frac{\partial}{\partial x} + \upsilon_2 \frac{\partial}{\partial y}\right)^2 + \epsilon^4 \frac{\partial^2}{\partial \tau^2} - \epsilon^3 \left[2\left(\upsilon_1 \frac{\partial}{\partial x} + \upsilon_2 \frac{\partial}{\partial y}\right) \frac{\partial}{\partial \tau}\right], \quad (7)$$

$$\frac{\partial^2}{\partial n^2} = \epsilon \frac{\partial^2}{\partial x^2}, \quad \frac{\partial^2}{\partial m^2} = \epsilon \frac{\partial^2}{\partial y^2}. \quad (8)$$

By inserting Eqs. (5)–(8) into Eq. (4) and collecting terms of the same order in ϵ, we find that the coefficient proportional to lowest order (ϵ^2) gives

$$(\upsilon_1^2 - u_{01}^2) \frac{\partial^2 \psi}{\partial x^2} + (\upsilon_2^2 - u_{02}^2) \frac{\partial^2 \psi}{\partial y^2} + 2\upsilon_1 \upsilon_2 \frac{\partial^2 \psi}{\partial x \partial y} = 0. \quad (9)$$

In the next order, after integration and setting the constant of integration to zero, we obtain

$$\frac{\partial \psi}{\partial \tau} + \left(\upsilon_1 \frac{\partial}{\partial x} + \upsilon_2 \frac{\partial}{\partial y} - 2\epsilon \frac{\partial}{\partial \tau}\right) \times \left(\alpha \psi^2 + C_{r1} \frac{\partial^2 \psi}{\partial x^2} + C_{r2} \frac{\partial^2 \psi}{\partial y^2}\right) = 0. \quad (10)$$

The solutions of Eq. (2) can be obtained by solving Eqs. (9) and (10). To this end, we define the single variable

$$z = x\cos(\theta) + y\sin(\theta) - \upsilon_c \tau, \quad (11)$$

where υ_c is the front wave velocity and θ is the propagation direction of the wave relative to the x-direction. By considering this definition, equation (9) becomes the following ordinary differential equation:

$$[(\upsilon_1^2 - u_{01}^2)\cos^2(\theta) + (\upsilon_2^2 - u_{02}^2)\sin^2(\theta) + 2\upsilon_1 \upsilon_2 \cos(\theta)\sin(\theta)] \frac{\partial^2 \psi}{\partial z^2} = 0. \quad (12)$$

This last equation is identically verified if we express υ_1 and υ_2 in terms of θ according to

$$\upsilon_1 = \upsilon_0 \cos(\theta), \quad \upsilon_2 = \upsilon_0 \sin(\theta), \quad (13)$$

with

$$\upsilon_0 = \sqrt{u_{01}^2 \cos^2(\theta) + u_{01}^2 \sin^2(\theta)}.$$

Inserting Eqs. (11) and (13) into Eq. (10), then integrating and setting the constant of integration to zero lead to

$$-\upsilon_c \psi + \upsilon_0 \alpha \psi^2 + \upsilon_0 C_r \frac{\partial^2 \psi}{\partial z^2} + \epsilon \left(2\upsilon_c \alpha \psi^2 + 2\upsilon_c C_r \frac{\partial^2 \psi}{\partial z^2}\right) = 0, \quad (14)$$

where $C_r = C_{r1}\cos^2(\theta) + C_{r2}\sin^2(\theta)$.

3. Dynamical studies and sine-Gordon expansion-method

3.1. Dynamical studies

Now, we turn our attention to the dynamical studies of the above characteristic ODE of the network. Various solutions of this equation can be obtained depending on the value of the parameter υ_c. When $C_r(\upsilon_0 + 2\epsilon\upsilon_c) \neq 0$, equation (14) can be reduced to a two-dimensional dynamical system

$$\begin{cases} \frac{d\psi}{dz} = \phi, \\ \frac{d\phi}{dz} = \frac{\psi}{C_r(\upsilon_0 + 2\epsilon\upsilon_c)}(\upsilon_c - \alpha(\upsilon_0 + 2\epsilon\upsilon_c)\psi). \end{cases} \quad (15)$$

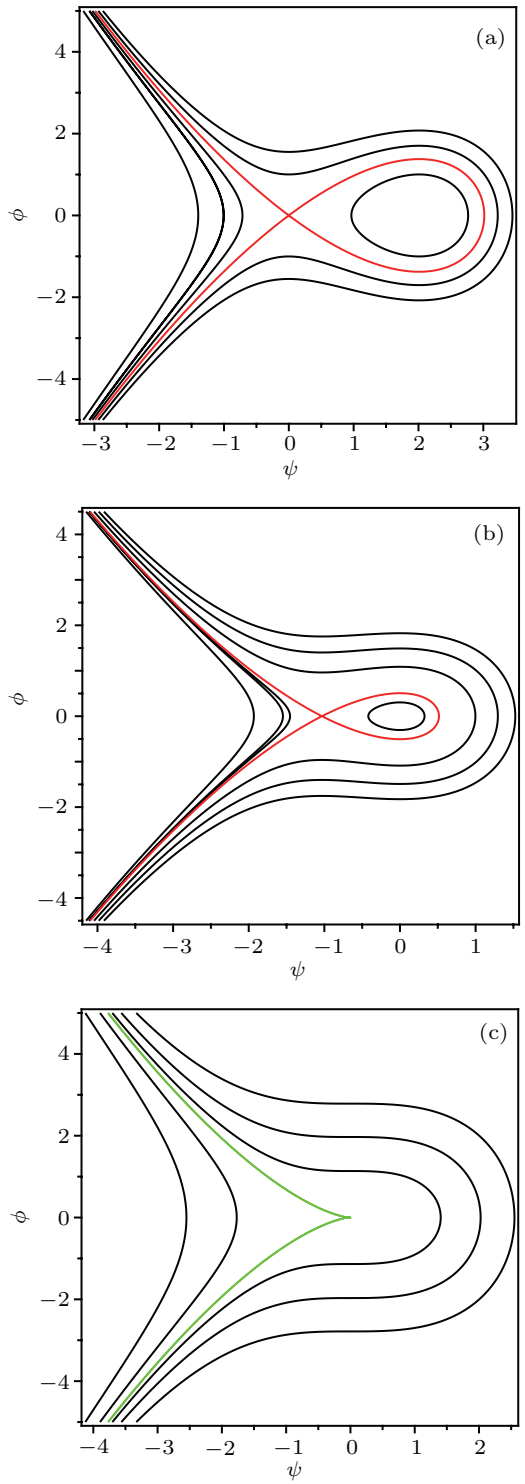


Fig. 3. (color online) The phase portraits of system (15) in the (ψ, ψ')-phase plane for $u_{01} = u_{02} = 2.5786 \times 10^6$ rad/s, $C_{r1} = C_{r2} = 0.3$, $\theta = \pi/32$, $\alpha = 0.21$ V^{-1}, $\beta = 0$: (a) $\upsilon_c > 0$ or $\upsilon_c < -\upsilon_0/2\epsilon$, (b) $-\upsilon_0/2\epsilon < \upsilon_c < 0$, (c) $\upsilon_c = 0$.

System (15) has a first integral defined as

$$\left(\frac{\partial \psi}{\partial z}\right)^2 + U(\psi) = K, \tag{16}$$

where K is an integral constant and $U(\psi)$ is an effective potential defined by

$$U(\psi) = -\frac{\upsilon_c}{C_r(\upsilon_0 + 2\epsilon\upsilon_c)}\psi^2 + \frac{2\alpha}{3C_r}\psi^3. \tag{17}$$

We observe that system (15) has several singular points depending on the value of the front wave velocity υ_c. In fact, $O(0,0)$ is always the equilibrium point of system (15) independently of the value and sign of this parameter. Equation (15) has one additional equilibrium point $A_1(\frac{\upsilon_c}{\alpha(\upsilon_0+2\epsilon\upsilon_c)}, 0)$. When $\upsilon_c > 0$ or $\upsilon_c < -\frac{\upsilon_0}{2\epsilon}$, A_1 is a center and $O(0,0)$ is a saddle point. For $-\frac{\upsilon_0}{2\epsilon} < \upsilon_c < 0$, the natures of these equilibrium points change: $O(0,0)$ becomes a center and A_1 is a saddle point. This analysis is confirmed by the phase plane plot of the system sketched in Fig. 3.

On the preceding figure (Fig. 3), we distinguish the following types of orbits: (i) a homoclinic orbit (red curve) which corresponds to a pulse soliton or bright solitary waves (BSW) solution of Eq. (10); (ii) periodic orbits (closed black curve) which correspond to periodic traveling wave solutions of equation (10). From these figures, we summarize crucial conclusions as follows. (i) If $\upsilon_c \neq 0$, system (15) always has an homoclinic orbit which is asymptotic to the saddle and encloses the center. In this case, there also exists a family of periodic orbits which enclose the center and fill up the interior of the homoclinic orbit. (ii) When $\upsilon_c = 0$, the equilibrium point $O(0,0)$ is a cusp.

3.2. The sine-Gordon expansion-method

In this subsection, we present the sine-Gordon expansion method which will later be utilized to investigate the solitary waves of the coupled electric transmission line. This method is based on the sine-Gordon equation and a traveling wave transformation.[64–66]

In fact, consider a nonlinear partial differential equation (NLPDE) with two independent variables x and t

$$H(U_t, U_x, U_{xx}, U_{tt}, \ldots) = 0. \tag{18}$$

In general, the left hand side of Eq. (18) is a polynomial in U and its various derivatives. Assuming that $U(x,t) = U(\xi)$, $\xi = k_1 x - \upsilon_c t$, where k_1 and υ_c are constants to be determined later, then equation (18) is reduced to an ordinary differential equation

$$G\left(U, \frac{\mathrm{d}U}{\mathrm{d}\xi}, \frac{\mathrm{d}^2U}{\mathrm{d}\xi^2}, \ldots\right) = 0, \tag{19}$$

where G is a polynomial of U and its various derivatives.

We consider that the sought solution can be expressed as follows:

$$U(\xi) = \sum_{i=1}^{I_m} \tanh^{i-1}(\xi)\,(a_i \operatorname{sech}(\xi) + b_i \tanh(\xi)) + a_0. \tag{20}$$

According to Refs. [68]–[70], equation (20) can be rewritten as

$$U(w) = \sum_{i=1}^{I_m} \cos^{i-1}(w)\,(a_i \sin(w) + b_i \cos(w)) + a_0, \tag{21}$$

where the function $w(\xi) = U(\xi)/2$ satisfies the following relation:

$$w' = \sin(w). \tag{22}$$

Equation (22) is variables separable, and we obtain the following two significant equations upon solving it:

$$\sin(w) = \sin(w(\xi)) = \frac{2p\exp(\xi)}{p^2\exp(2\xi)+1}|_{p=1} = \mathrm{sech}(\xi), \tag{23}$$

$$\cos(w) = \cos(w(\xi)) = \frac{p^2\exp(2\xi)-1}{p^2\exp(2\xi)+1}|_{p=1} = \tanh(\xi). \tag{24}$$

The parameter I_m is, in most cases, a positive integer that can be determined by considering the homogeneous balance between the highest order derivative and the highest order nonlinear terms appearing in ODE (19). Collecting and setting the coefficients of terms of the form $\sin^i(w)\cos^j(w)$ to zero yield a system of coupled nonlinear algebraic equations. Solving this system using Maple gives the values of a_i, b_i, a_0, k_1, and υ_c. Finally, upon substituting these values in Eq. (20), we obtain the traveling wave solutions to Eq. (19).

4. Exact solution of Eq. (14)

4.1. Implementation of the sine-Gorgon method

Now we focus our attention on the derivation of the bright solution of the two-dimensional partial differential equation (4). To this end, we introduce the variable $\xi = \mu z$ and equation (14) becomes

$$\mu^2\frac{\partial^2\psi}{\partial\xi^2} - A\psi + B\psi^2 = 0, \tag{25}$$

in which

$$A = \frac{\upsilon_c}{C_r(\upsilon_0+2\epsilon\upsilon_c)}, \quad B = \frac{\alpha}{C_r}. \tag{26}$$

On balancing the nonlinear term ψ^2 and the highest order derivative term ψ'' in Eq. (25), we find that $I_m = 2$. So, we may express the solutions of this equation in the form

$$\begin{aligned} U(w) &= a_1\sin(w) + b_1\cos(w) + a_2\cos(w)\sin(w) \\ &\quad + b_2\cos(w)^2 + a_0, \\ U''(w) &= a_1\cos^2(w)\sin(w) - a_1\sin^3(w) \\ &\quad - 2b_1\cos(w)\sin^2(w) - 5a_2\cos(w)\sin^3(w) \\ &\quad + a_2\cos^3(w)\sin(w) - 4b_2\cos(w)^2\sin^2(w) \\ &\quad + 2b_2\sin^4(w). \end{aligned} \tag{27, 28}$$

Substituting Eqs. (27) and (28) in into Eq. (26), and equating the coefficients of each power of $\sin^i(w)\cos^j(w)$ to zero, we obtain a system of algebraic equations of the parameters a_0, a_1, a_2, b_1, b_2, and μ, i.e.,

$$\begin{aligned} &\text{constant} && : 2\mu^2a_2 + Ba_0^2 - Aa_0 + Bb_1^2 = 0, \\ &\sin(w) && : 2Ba_0b_1 - Ab_1 - \mu^2b_1 = 0, \\ &\cos(w) && : 2Ba_0a_1 - Aa_1 - 2\mu^2a_1 + 2Bb_1b_2 = 0, \\ &\cos(w)\sin(w) && : -Ab_2 + 2Ba_0b_2 + 2Ba_1b_1 - 5\mu^2b_2 = 0, \\ &\cos^2(w) && : 2Ba_0a_2 - Aa_2 - 8\mu^2a_2 \\ &&& \quad -Bb_1^2 + Ba_1^2 + Bb_2^2 = 0, \\ &\cos^2(w)\sin(w) && : 2\mu^2b_1 + 2Ba_1b_2 + 2Ba_2b_1 = 0, \\ &\cos^3(w) && : 2Ba_1a_2 + 2\mu^2a_1 - 2Bb_1b_2 = 0, \\ &\cos^3(w)\sin(w) && : 6\mu^2b_2 + 2Ba_2b_2 = 0, \\ &\cos^4(w) && : 6\mu^2a_2 + Ba_2^2 - Bb_2^2 = 0. \end{aligned} \tag{29}$$

It appears that there are three more equations than the six variables sought for. Such a large number of coupled nonlinear algebraic equations can be obviously very challenging for human manipulation. On the contrary, computer algebra tools such as Maple, Mathematica, or MuPAD are very powerful for such tasks, especially as these equations are all polynomial. For the explicit solutions that are of interest to us in this paper, and disregarding the trivial (constant) solutions, we find with the help of Maple that they depend on the combination of the physical parameters as considered below.

Case I The parameters are

$$a_0 = \frac{3A}{2B}, \quad a_2 = -\frac{3A}{2B}, \quad \mu = \frac{1}{2}\sqrt{A}, \quad a_1 = b_1 = b_2 = 0. \tag{30}$$

With these values, we have

$$\psi(x,y,t) = \frac{3A}{2B}\mathrm{sech}^2\left[\frac{1}{2}\sqrt{A}(x\cos(\theta) + y\sin(\theta) - \upsilon_c t)\right]. \tag{31}$$

A graphical representation of the corresponding solutions is given in Fig. 4 for precise values of parameters. The obtained solution is a bright pulse soliton.

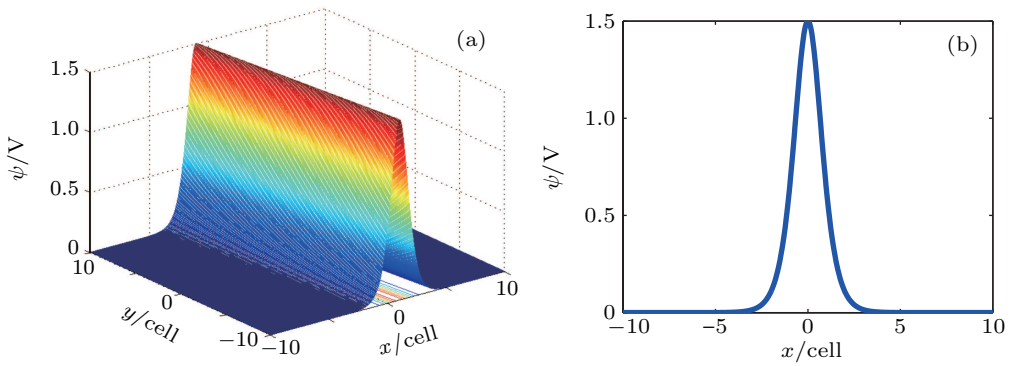


Fig. 4. (color online) The 3D and 2D bright solutions of Eq. (31) for $A = 1$, $B = 1$, $\theta = \pi/32$, $t = 0$, $-10 < x < 10$: (a) $-10 < y < 10$, (b) $y = 0$.

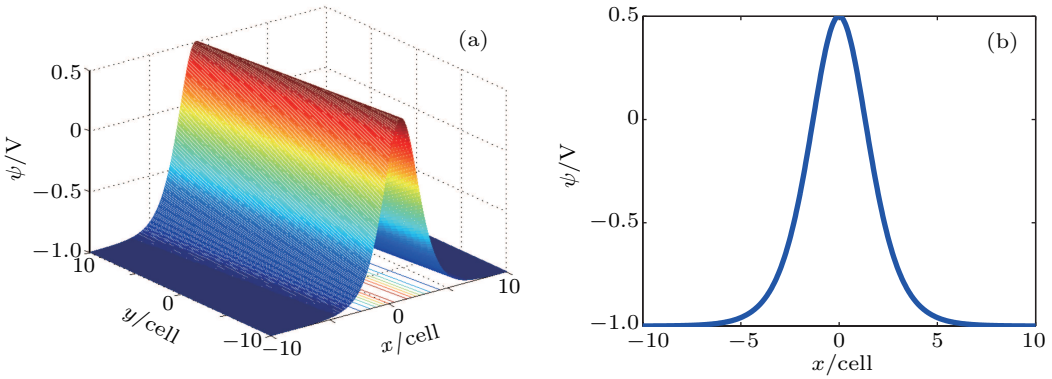


Fig. 5. (color online) The 3D and 2D bright solutions of Eq. (33) for $A=-1$, $B=1$, $\theta=\pi/32$, $t=0$, $-10<x<10$: (a) $-10<y<10$, (b) $y=0$.

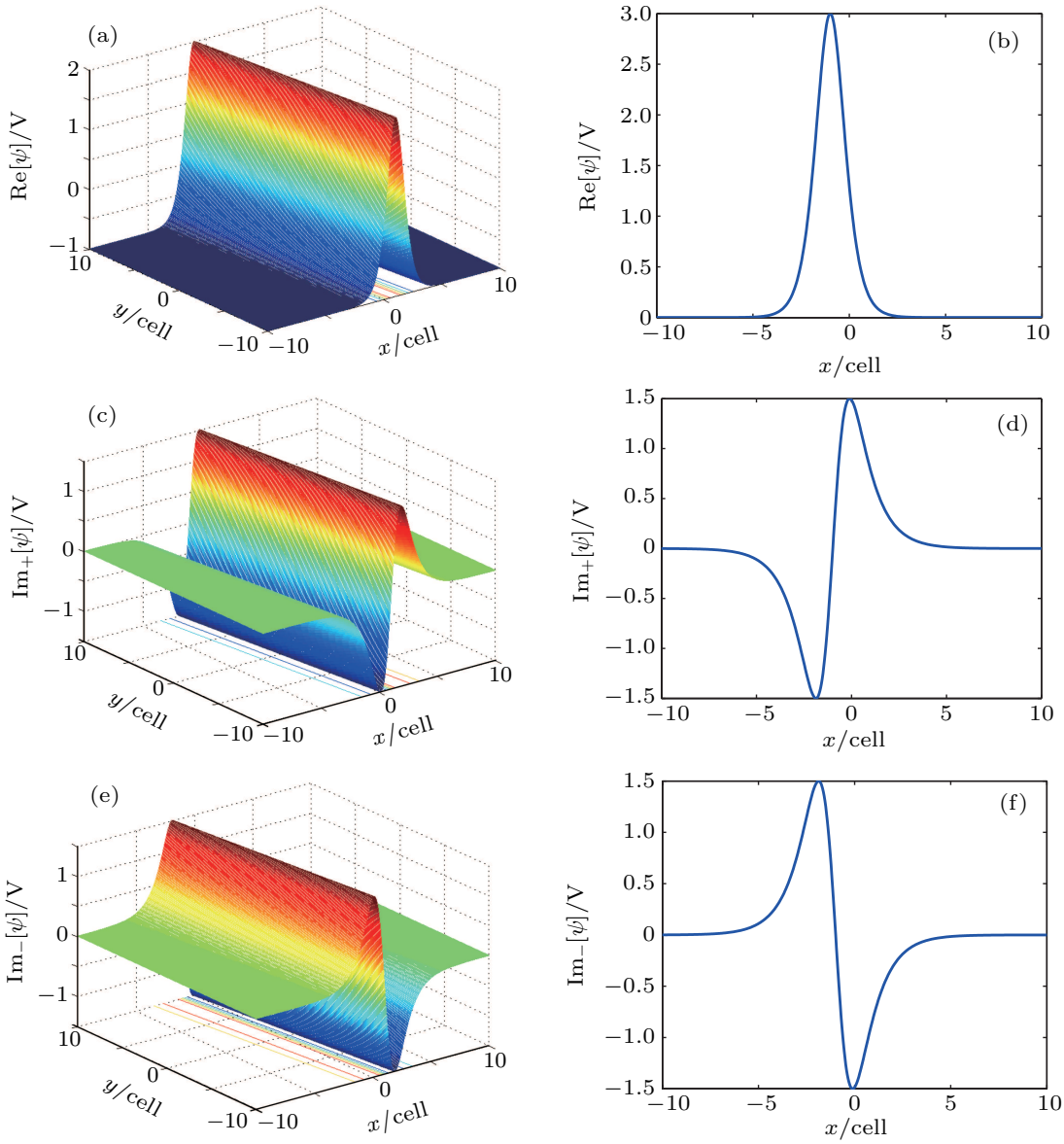


Fig. 6. (color online) The 3D and 2D bright and breathers solutions of Eq. (35) for $A=1$, $B=1$, $\theta=\pi/32$, $t=0$, $-10<x<10$: (a), (c), (e) $-10<y<10$; (b), (d), (f) $y=10$.

Case II The parameters are

$$a_0=-\frac{A}{2B},\quad a_2=\frac{3A}{2B},\quad \mu=\frac{1}{2}\sqrt{-A},\quad a_1=b_1=b_2=0. \tag{32}$$

We obtain the following solution:

$$\psi(x,y,t)=\frac{3A}{2B}\left[\tanh^2\left[\frac{1}{2}\sqrt{-A}(x\cos(\theta)+y\sin(\theta)-\upsilon_c t)\right]-\frac{1}{3}\right]. \tag{33}$$

A graphical representation of the corresponding solution is given in Fig. 5 for some values of the parameters. The obtained solution is a grey soliton.

Case III The parameters are

$$a_0 = \frac{3A}{B}, \quad a_2 = -\frac{3A}{B}, \quad b_2 = \pm \mathrm{i}\frac{3A}{B}, \\ \mu = \sqrt{A}, \quad a_1 = b_1 = 0, \tag{34}$$

which leads to

$$\psi(x,y,t) = \frac{3A}{B}\operatorname{sech}^2\left[\sqrt{A}(x\cos(\theta)+y\sin(\theta)-\upsilon_c t)\right] \\ \pm \mathrm{i}\frac{3A}{B}\tanh\left[\sqrt{A}(x\cos(\theta)+y\sin(\theta)-\upsilon_c t)\right] \\ \times \operatorname{sech}\left[\sqrt{A}(x\cos(\theta)+y\sin(\theta)-\upsilon_c t)\right]. \tag{35}$$

Graphical representation of this solution is given in Fig. 6 for selected values of parameters. The obtained solutions are bright and breather solitons.

Case IV The parameters are

$$a_0 = -\frac{2A}{B}, \quad a_2 = \frac{3A}{B}, \quad b_2 = \pm \mathrm{i}\frac{3A}{B}, \\ \mu = \sqrt{-A}, \quad a_1 = b_1 = 0, \tag{36}$$

which leads to

$$\psi(x,y,t) = \frac{3A}{B}\left[\tanh^2\left[\sqrt{-A}(x\cos(\theta) \right.\right. \\ \left.\left. +y\sin(\theta)-\upsilon_c t)\right]-\frac{2}{3}\right] \\ \pm \mathrm{i}\frac{3A}{B}\tanh\left[\sqrt{-A}(x\cos(\theta)+y\sin(\theta)-\upsilon_c t)\right] \\ \times \operatorname{sech}\left[\sqrt{-A}(x\cos(\theta)+y\sin(\theta)-\upsilon_c t)\right]. \tag{37}$$

A graphical representation of the corresponding solution is given in Fig. 7. The obtained solutions are grey soliton and breather solutions.

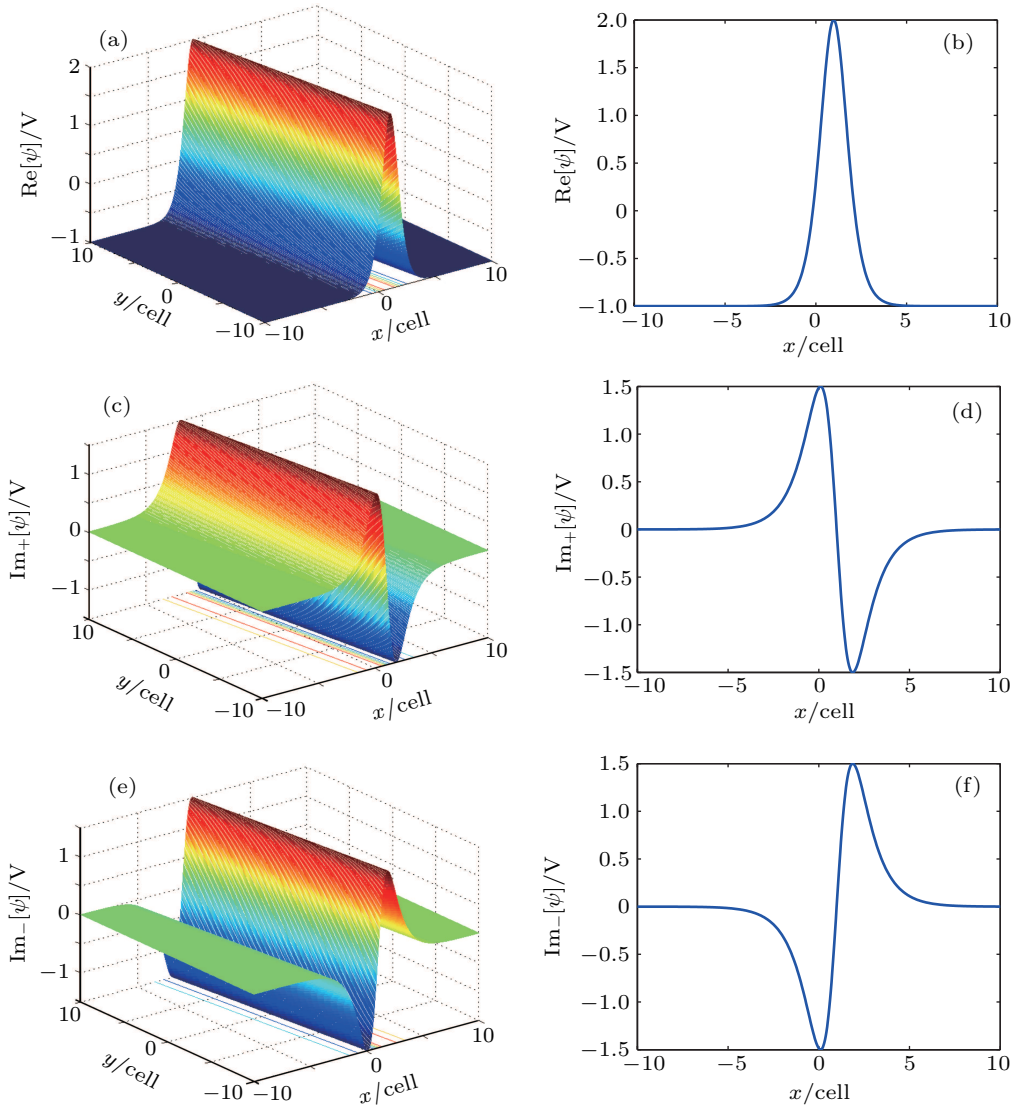


Fig. 7. (color online) The 3D and 2D bright and breathers solutions of Eq. (31) for $A=-1$, $B=1$, $\theta=\pi/32$, $t=0$, $-10<x<10$: (a), (c), (e) $-10<y<10$; (b), (d), (f) $y=10$.

4.2. Supplementary solutions

This subsection is devoted to the computation of other exact solutions of Eq. (14) which correspond to bounded traveling wave solutions of Eq. (1). Equation (16) can be written in the form

$$\left(\frac{\partial\psi}{\partial z}\right)^2 = -\frac{2B}{3}\left(\psi^3 - \frac{3A}{2B}\psi^2 - \frac{3K}{2B}\right). \tag{38}$$

Let

$$f(\psi) = \psi^3 - \frac{3A}{2B}\psi^2 - \frac{3K}{2B}, \tag{39}$$

$$\Delta = \left(\frac{A^2+6KB^2}{8B^3}\right)^2 - \left(\frac{A}{2B}\right)^6. \tag{40}$$

If $\Delta < 0$, $f(\phi)$ admits three real roots ψ_1, ψ_2, and ψ_3 with $\psi_1 \geq \psi_2 \geq \psi_3$. In this case, we have

$$f(\psi) = (\psi-\psi_1)(\psi-\psi_2)(\psi-\psi_3). \tag{41}$$

From Eq. (41), we obtain

$$\psi_1\psi_2\psi_3 = \frac{3K}{2B},$$
$$\psi_1+\psi_2+\psi_3 = \frac{3A}{2B},$$
$$\psi_1\psi_2+\psi_1\psi_3+\psi_2\psi_3 = 0. \tag{42}$$

By using the first equation (38), one obtains

$$\frac{\mathrm{d}\psi}{\sqrt{(\psi_1-\psi)(\psi-\psi_2)(\psi-\psi_3)}} = \sqrt{\frac{2B}{3}}\mathrm{d}z. \tag{43}$$

The exact solutions of Eq. (14) are obtained from the results of Eq. (43). Some transformations[77] lead to

$$\psi(x,y,t) = \psi_2 + (\psi_1-\psi_2)\,\mathrm{cn}^2\left[\sqrt{\frac{B(\psi_1-\psi_3)}{6}}(x\cos(\theta) + y\sin(\theta) - \upsilon_c t), \frac{\psi_1-\psi_2}{\psi_1-\psi_3}\right]. \tag{44}$$

The last equation of Eq. (42) clearly shows that these roots do not all have the same sign. Thus, we have the following two situations: (i) $\psi_1 > 0$, $\psi_2 > 0$, $\psi_3 < 0$; and (ii) $\psi_1 > 0$, $\psi_2 < 0$, $\psi_3 < 0$. The graphs of Eq. (44) for these two situations are shown in Figs. 8(a) and 8(b), respectively, which are the periodic wave solutions of Eq. (14).

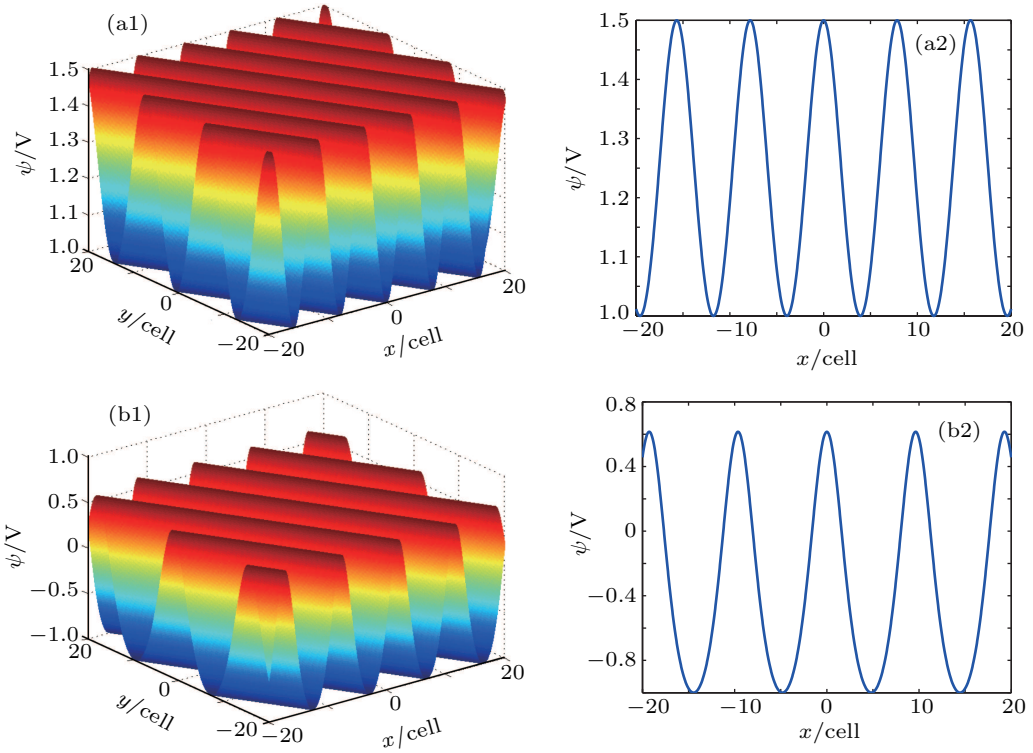


Fig. 8. (color online) The 3D and 2D periodic solutions of Eq. (44) for $B = 0.7$, $\theta = \pi/6$, $t = 0$, $-20 < x < 20$: (a1), (b1) $-20 < y < 20$; (a2), (b2) $y = 0$. (a) $\psi_3 = -0.6$, $\psi_2 = 1$, and $\psi_1 = 1.5$. (b) $\psi_3 = -1.6$, $\psi_3 = -1$, and $\psi_1 = 0.6154$.

We remark that, for $\psi_2 = \psi_3 = 0$ and $K = 0$, we have $\psi_1 = \frac{3A}{2B}$ and solution (44) is identical to the bell profile solitary wave solution (31). Similarly, for $\psi_2 = \psi_3 = \frac{A}{B}$ and $K = -\frac{A^3}{3B^2}$, we have $\psi_1 = -\frac{A}{2B}$, and solution (44) is identical to the bell profile solitary wave solution (33).

5. Physically exploitable solutions in the particular case of the electrical network

The results obtained in this paper are bright soliton, grey soliton, breathers, and periodic solutions. These solutions are used for the information transmission through the electrical

lattice and can also help to explain the dynamics of many other discrete lattices like a chain of atoms. Particulary, for the case of the two-dimensional nonlinear electrical network in Fig. 1, we have the following exploitable results.

5.1. Situation 1: $\upsilon_c > 0$ or $\upsilon_c < -\upsilon_0/2\epsilon$ ($A > 0$ and $B > 0$)

In this case, both bell-shaped soliton as well as periodic solitary waves can be propagated in the network. For $K = 0$, the explicit expression of voltage corresponding to the pulse-like signal is given by

$$V_{n,m}(t) = V_0 \operatorname{sech}^2\left[\mu_0\left(n\cos(\theta) + m\sin(\theta) - \upsilon_{p1}t\right)\right], \quad (45)$$

with $\upsilon_{p1} = \upsilon_0\left(1 + \frac{2\alpha V_0}{3-4\alpha V_0}\right)$ and $\mu_0 = \sqrt{\frac{\alpha V_0}{6C_r}}$; υ_0 and C_r are defined by Eqs. (13) and (14), respectively. This expression involves four main quantities, including the amplitude V_0, the speed υ_{p1}, the reduced propagation direction θ, and the width $L_s = 1/\mu_0$. From the expression of υ_{p1}, it appears that the soliton can effectively exist for $V_0 \neq \frac{3}{4\alpha}$; and that of μ_0 shows clearly that the width originates from the quadratic nonlinearity and crucially depends on the signal's amplitude V_0. It is also worth to notice that the envelope velocity of the pulse is dependent on the amplitude V_0 of the signal. For positive front wave velocity υ_c, the envelope velocity increases with the amplitude V_0 and decrease in the contrary case. Thus, since the wave velocity is amplitude dependent, two adjacent pulse solitons of different amplitudes will interact in the network because they propagate at different speeds.

When $-\frac{A^3}{3B^2} < K < 0$, the explicit expression of voltage corresponding to the periodic signal voltage is given by

$$\begin{aligned} V_{n,m}(t) \;=\; & \epsilon\psi_2\left[1 + \frac{\psi_2}{\psi_2+\psi_3}\,\mathrm{cn}^2\right. \\ & \times\left(\sqrt{\frac{-\epsilon B\psi_3(2\psi_2+\psi_3)}{6(\psi_2+\psi_3)}}(n\cos(\theta) + m\sin(\theta)\right. \\ & \left.\left. - (\upsilon_0 + \epsilon\upsilon_c)t), \frac{\psi_2(\psi_2+2\psi_3)}{\psi_3(\psi_3+2\psi_2)}\right)\right], \end{aligned} \quad (46)$$

in which

$$\begin{aligned} \psi_{2,3} &= \frac{A}{2B} - \frac{C+D}{2} \pm \mathrm{i}\frac{\sqrt{3}(C-D)}{2}, \\ C &= \left(\frac{A^3+6KB^2}{8B^3} + \sqrt{\Delta}\right)^{1/3}, \\ D &= \left(\frac{A^3+6KB^2}{8B^3} - \sqrt{\Delta}\right)^{1/3}. \end{aligned} \quad (47)$$

5.2. Situation 2: $-\upsilon_0/2\epsilon < \upsilon_c < 0$ ($A < 0$ and $B > 0$)

Here, the types of waves supported by the network are periodic and grey solitary waves. The former exists for $0 < K < -\frac{A^3}{3B^2}$ and is also described by Eq. (46). The grey soliton signal voltage is obtained for $K = -\frac{\upsilon_c^3}{3\alpha^2 C_r(\upsilon_0+2\epsilon\upsilon_c)^3}$, and reads

$$V_{n,m}(t) \;=\; \frac{V_0}{3} - V_0\tanh^2[\mu_0(n\cos(\theta) + m\sin(\theta) - \upsilon_{p2}t)], \quad (48)$$

with $\upsilon_{p2} = \upsilon_0\left(1 - \frac{2\alpha V_0}{3+4\alpha V_0}\right)$ and υ_0 and C_r defined by Eqs. (13) and (14), respectively. It is also described by the same four parameters as in the case of bright soliton of the preceding situations.

6. Conclusion

We have investigated the transverse wave solutions in a system of coupled nonlinear partial differential equations that was earlier shown to govern the dynamics of waves in a coupled nonlinear inductor-capacitor network. Firstly, using the dynamical studies we found that the phase portrait of the system admits an homoclinic orbit and periodic orbits which respectively correspond to a bright soliton and periodic wave solutions of the equation governing the network. Next, via the sine-Gordon expansion-method and direct integration, we obtained all traveling wave solutions of these coupled equations such as complex, elliptic, and hyperbolic function solutions. The two- and three-dimensional graphics of all obtained solutions in this work are given. Finally, some of these solutions that are physically exploitable in the particular case of the network considered (Fig. 1) are presented. These solutions are used for the information transmission through the electrical lattice and can also help to explain the dynamics of many other physical systems. The sine-Gordon expansion-method used here is powerful and can be also applied to other nonlinear equations in mathematical physics.

References

[1] Lorin E, Lytova M, Memarian A and Bandrauk A D 2015 *J. Phys. A: Math. Theor.* **48** 105201
[2] Maucher F, Buccoliero D, Skupin S, Grech M, Desyatnikov A S and Krolikowski W 2009 *Optical and Quantum Electronics* **41** 337
[3] Alejandro B A, Gadi F and Boaz I 2004 *Physica D* **189** 277
[4] Alidou M, Kenfack-Jiotsa A and Kofane T C 2006 *Chaos Solitons Fract.* **27** 914
[5] Nath R, Pedri P and Santos L 2008 *Phys. Rev. Lett.* **101** 210402
[6] Kinstrie C J and Bingham R 1989 *Physics of Fluids B* **1** 230
[7] Ndjoko P B, Bilbault J M, Binczak S and Kofane T C 2012 *Phys. Rev. E* **85** 011916
[8] Lu B B, Deng Y P and Tian Q 2010 *Chin. Phys. B* **19** 026302
[9] Xu Q and Qiang T 2009 *Chin.Phys.Lett.* **26** 070501
[10] Cui W N, Li H X, Sun M and Zhu Y Y 2016 *Chin.Phys.Lett.* **33** 124101
[11] Huang L F, Li Y L, Ni M Y, Wang X L, Zhang G R and Zeng Z 2009 *Acta Phys. Sin.* **58** 306
[12] Xu Q and Tian Q 2013 *Chin. Phys. B* **22** 086302
[13] Xu Q and Tian Q 2010 *Chin.Phys.Lett.* **27** 020505
[14] Wang X J, Liu J F, Luo Y F and Li S 2010 *Chin.Phys.Lett.* **27** 016301
[15] Xie H, Zhao Y W, Liu T, Dong Z Y, Yang J and Liu J M 2015 *Chin. Phys. B* **24** 107704
[16] Chen A L, Liang T L and Wang Y S 2015 *Chin. Phys. B* **24** 066101
[17] Zhou K Y and Guo Z Y 2010 *Chin. Phys. B* **19** 014201
[18] Zhu Q G, Dong X Y, Wang C F, Wang N and Chen W D 2015 *Acta Phys. Sin.* **64** 034209
[19] Chen A L, Liang T L and Wang Y S 2014 *Acta Phys. Sin.* **63** 036101
[20] Pelap F B, Kofané C T, Flytzanis N and Remoissenet M 2001 *J. Phys. Soc. Jpn.* **70** 2568

[21] Pelap F B and Faye M M 2005 *Nonlinear Oscillations* **8** 513
[22] Kengne E and Liu W M 2006 *Phys. Rev. E* **73** 026603
[23] Yemélé D, Marquié P and Bilbault J M 2003 *Phys. Rev. E* **68** 016605
[24] Pelap F B and Faye M M 2007 *J. Phys. Soc. Jpn.* **76** 074602
[25] Yamgoué S B, Pelap F B 2016 *Phys. Lett. A* **380** 2017
[26] Wang Z B, Wu Z Z and Gao C 2015 *Chin. Phys. B* **24** 028503
[27] Guoying Z, Feng T and Weizhong C 2016 *Chin. Phys. B* **25** 044101
[28] Peyrard M and Dauxois T 2004 *Physique des solitons*, CNRS EDITIONS, 15, rue Malebranche, 75005 Paris
[29] Li J and Jiang L 2015 *International Journal of Bifurcation and Chaos* **25** 1550016
[30] Wang Z and Tang S 2009 *Commun. Nonlinear Sci. Numer. Simulat.* **14** 2018
[31] Li J and Qiao Z 2013 *Journal of Mathematical Physics* **54** 123501
[32] Cui W N, Zhu Y Y, Li H X and Liu S M 2010 *Chin.Phys.Lett.* **27** 114101
[33] Ding D J , Jin D Q and Dai C Q 2017 *Thermal Science* **21** 1701
[34] Abdel-Gawad H I and Tantawy M 2017 *Indian J. Phys.* **91** 671
[35] Wang Y Y, Chen L, Dai C Q, Zheng J and Fan Y 2017 *Nonlinear Dynamics* **90** 1269
[36] Manafian J and Lakestani M 2018 *Eur. Phys. J. Plus* **133** 119
[37] Yakada S, Yaouba A, Gambo B, Doka S Y and Kofane T C 2017 *Nonlinear Dyn.* **87** 2435
[38] Kenfack-Jiotsa A and Tala-Tebue E 2011 *J. Phys. Soc. Jpn.* **80** 034003
[39] Kenmogne F, Yemélé D, Kengne J and Ndjanfang D 2014 *Phys. Rev. E* **90** 052921
[40] Dai C Q, Zhou G Q, Chen R P, Lai X J and Zheng J 2017 *Nonlinear Dynamics* **88** 2629
[41] Wang Y Y, Dai C Q, Xu Y Q, Zheng J and Fan Y 2018 *Nonlinear Dynamics* **92** 1261
[42] Ma W X, Yong X and Zhang H Q 2018 *Comput. Math. Appl.* **75** 289
[43] Zhao H Q and Ma W X 2017 *Comput. Math. Appl.* **74** 1399
[44] Zhang J B and Ma W X 2017 *Comput. Math. Appl.* **74** 591
[45] Ma W X and Zhou Y 2018 *Journal of Differential Equations* **264** 2633
[46] Liu W J, Liu M, OuYang Y, Hou H, Ma G, Lei M and Wei Z 2018 *Nanotechnology* **29** 174002
[47] Ma W X and Fuchssteiner B 1996 *Iternational Journal of Non-Linear Mechanics* **31** 329
[48] Ma W X and Lee J H 2009 *Chaos, Solitons and Fractals* **42** 1356
[49] Akbari M 2014 *Quantum Physics Letters* **3** 33
[50] Tala-Tebue E, Tsobgni-Fozap D C, Kenfack-Jiotsa A and Kofane T C 2014 *Eur. Phys. J. Plus* **129** 1
[51] Saidou A, Alidou M, Ousmanou D and Yamigno D S 2014 *Chin. Phys. B* **23** 120506
[52] Islam S R 2015 *World Applied Sciences Journal* **33** 659
[53] Zayed-Elsayed M E, Amer-Yasser A and Shohib-Reham M A 2015 *Scientific Research and Essays* **10** 218
[54] Kumar H and Chand F 2014 *Journal of Theoretical and Applied Physics* **8** 1
[55] Li J and Chen F 2015 *International Journal of Bifurcation and Chaos* **25** 1550045
[56] Li J and Jiang L 2015 *International Journal of Bifurcation and Chaos* **25** 1550016
[57] Tala-Tebue E, Djoufack Z I, Fendzi-Donfack E, Kenfack-Jiotsa A and Kofané T C 2016 *Optik* **127** 11130
[58] El-Wakil S A and Abdou M A 2008 *Nonlinear Analysis: Theory, Methods & Applications* **68** 235
[59] Manafian J and Lakestani M 2016 *Optik* **127** 9603
[60] Marinca V and Herişanu N 2011 *Mathematical and Computer Modelling* **53** 604
[61] Salas A H 2014 *Applied Mathematical Sciences* **8** 8781
[62] Salas A H and Castillo J E 2014 *Visión Electrónica: algo más que un estado sólido* **8** 46
[63] Ningning Y, Yuchao H, Chaojun W, Rong J and Chongxin L 2017 *Chin. Phys. B* **26** 080503
[64] Yan C 1996 *Phys. Lett. A* **22** 77
[65] Yan Z 1999 *Phys. Lett. A* **252** 291
[66] Baskonus H M 2016 *Nonlinear Dyn.* **86** 177
[67] Zhang B, Zhang X L and Dai C Q 2017 *Nonlinear Dynamics* **87** 2385
[68] Baskonus H M, Sulaiman T A and Bulut H 2017 *Indian J. Phys.* **135** 327
[69] Ilhan O A, Sulaiman T A, Bulut H and Baskonus H M 2018 *Eur. Phys. J. Plus* **133** 27
[70] Bulut H, Sulaiman T A and Baskonus H M 2017 *Eur. Phys. J. Plus* **132** 459
[71] Remoissenet M 1999 *Waves Called Solitons* (3rd Edn.) (Berlin: Springer-Verlag)
[72] Marquié P, Bilbault J M and Remoissenet M 1994 *Phys. Rev. E* **49** 828
[73] Abdoulkary S, Mohamadou A and Beda T 2011 *Commun. Nonlinear Sci. Numer. Simulat.* **16** 3525
[74] Yamigno S D 2014 *Journal of Modern Physics* **5** 394
[75] Essimbi B Z and Jager D 2010 *Phys. Scr.* **81** 035801
[76] Duan W S 2004 *Europhys. Lett* **66** 192197
[77] Malwe Boudoue H, Nikolai A K, Mibaile J, Souleymanou A, Gambo B and Doka S Y 2018 *Eur. Phys. J. Plus* **133** 108